This material is posted here with permission of the IEEE. Such permission of the IEEE does not in any way imply IEEE endorsement of any of Helsinki University of Technology's products or services. Internal or personal use of this material is permitted. However, permission to reprint/republish this material for advertising or promotional purposes or for creating new collective works for resale or redistribution must be obtained from the IEEE by writing to pubs-permissions@ieee.org.

By choosing to view this document, you agree to all provisions of the copyright laws protecting it.

Manuscript to be published in IEEE Transaction on Component
and Packaging Technologies, with permission from IEEE.

Nucleation Kinetics and Solidification Temperatures of SnAgCu Interconnections during Reflow Process

H. Yu and J. K. Kivilahti, Fellow, IEEE
Laboratory of Electronics Production Technology
Helsinki University of Technology
PL 3000/P.O.Box 3000
FIN- 02015 HUT, Finland

ABSTRACT

The nucleation kinetics of β-Sn in liquid SnAgCu interconnections was simulated on the basis of nucleation theory. After evaluations of the compositions of liquid solder interconnections during reflow soldering, the free energy of nucleation can be calculated thermodynamically. Since homogeneous nucleation rate is very low, the mechanism that initiates solidification of interconnections is the heterogeneous nucleation at the Liq/Cu_6Sn_5 interface and the corresponding nucleation rates in interconnections are therefore simulated. Additional simulation of the nucleation rate in a tin droplet was also done to determine a critical range of nucleation rate. The contact angle for the heterogeneous nucleation was evaluated with the help of recent DSC measurements. The simulations allow us to evaluate the actual solidification temperature of interconnections, which is a fundamental parameter in studying the formation of solidified microstructure in solder interconnections. The variation of the solidification temperature with cooling rate, interconnection size, and morphology of intermetallic compounds is also discussed. Even though the actual solidification temperatures of interconnections depend on Ag-content, the supercooling range is shown to be fairly constant (18-20°C), which offers a possibility to predict the actual solidification temperature of interconnections via phase equilibria information.

INTRODUCTION

The importance of the reliability of soldered assemblies is increasing with the greater demands on functionality and performance of electronic equipment. Product reliability is especially important in portable electronics, because this more powerful and complex electronic equipment experiences, in addition to operational stresses, various kinds of mechanical, thermo-mechanical and chemical strains in the service environment. The reliability of soldered assemblies ultimately depends on the microstructures of the interconnections, the evolution of which is affected sensitively by temperature, stress and current density. Knowledge of the solidification structure formed in soldering operation is thus of primary importance in understanding how interconnection microstructures evolve with time. It is the as-solidified microstructure that determines the onset properties of solder interconnections. When the microstructure changes, the properties of the interconnections will change, both during reliability testing and product use [1]. There is good reason, therefore, to investigate the solidification of multicomponent solder interconnections by employing theoretical approaches involving concurrent use of thermal, thermodynamic and kinetic modelling tools and microstructural characterization techniques.

Solidification is the result of two successive steps: nucleation and growth of solid phase. In nucleation, the solder system has to overcome an energy barrier, and the liquid solder must supercool down to the so-called solidification temperature at which the solid phase first starts to form. The amount of supercooling, that is, the

difference between the actual and equilibrium solidification temperatures, depends on the nucleation kinetics. High-level supercooling can be achieved in tiny droplets. For example, supercooling up to 105°C has been observed in pure tin droplets with diameters ranging from 1μm to 10μm [2]. Since interconnections are very much smaller than typical bulk castings, their supercooling during the reflow soldering cannot be neglected. This has been confirmed by recent DSC measurements [3], which revealed that SnAgCu solder droplets in copper pans solidify at temperatures much lower than the liquidus temperature. It is important therefore to know the exact actual solidification temperatures of interconnections.

Although three phases form during the solidification of near-eutectic SnAgCu solders — β-Sn, Cu_6Sn_5 and Ag_3Sn — the amounts of Cu_6Sn_5 and Ag_3Sn are limited and more than 95 vol.% of the solidified interconnections is β-Sn, including both primary and eutectic tin. From this it can be concluded that the level of supercooling of interconnections is controlled by the kinetics of β-Sn nucleation.

On the basis of classical nucleation theory [4,5], we study the nucleation kinetics of β-Sn formation in SnAgCu interconnections and thus predict the actual solidification temperature of interconnections in this paper. This is necessary in studying the formation of cells, dendrites, and colonies as well as other microstructural units in as-solidified solder interconnections. Our aim is, by combining this analysis with those of the thermal and thermodynamic simulations that we presented earlier [6,7], to be able to predict and control solidification structures and so, ultimately, the reliability of solder interconnections.

LIQUID COMPOSITION OF INTERCONNECTIONS

Before we can analyze the kinetics of β-Sn nucleation, we need to know the liquid composition of interconnections. When a solder interconnection is melted during reflow soldering, the liquid spreads over the soldering pads on both component and printed wiring board. Intermetallic layers, such as Cu_6Sn_5 and Cu_3Sn, form rapidly at the interface between bulk solders, component metallizations and boards/metal finishes. The thickness of Cu_6Sn_5 layer increases with time but is limited to several microns, so the major part of the interconnections remains liquid. Massive solidification occurs only when β-Sn starts to form.

The Cu_6Sn_5 layer grows gradually before the massive solidification occurs during reflow soldering. According to the concept of local equilibrium, the liquid composition at the Liq/Cu_6Sn_5 interface should acquire such a value that the liquid is in local equilibrium with Cu_6Sn_5. This value is evidently not the original composition of solder interconnections.

During directional growth of a solid into a large amount of liquid, the composition in liquid varies continuously within the boundary layer at the front of the solid/liquid interface. The characteristic thickness of the boundary layer can be calculated as $2D/v$ [8], where v is the velocity of the moving solid/liquid interface and D is the diffusion coefficient of the solute atoms. For the growth of Cu_6Sn_5 occurring in reflow soldering, since the growth is parabolic [9] and the final thickness of Cu_6Sn_5 is typically several microns, the velocity of the Liq/Cu_6Sn_5 interface is less than 10^{-7} m/s. Further, since the diffusion coefficients of solute atoms in liquid are on the order of 10^{-9} m^2/s, the characteristic thickness of the boundary layer must be at least several centimeters, which significantly exceeds the sizes of both interconnections and DSC samples. Evidently, it means that solute atoms diffuse in interconnections rapidly enough to keep the liquid composition uniform. The compositions of the liquid

interconnections is therefore determined by the equilibrium between liquid and Cu_6Sn_5.

It follows that liquid compositions of interconnections vary with the temperature during reflow soldering. Fig. 1 plots the isothermal sections of the SnAgCu phase diagram calculated by using a thermodynamic databank system. [10] In order to evaluate the composition of the liquid before Sn nucleation, β-Sn has been suspended in the case of the metastable liquid being supercooled. The composition of the liquid being equilibrium with Cu_6Sn_5 lies on the boundary between the L and L+Cu_6Sn_5 regions in the diagram. Because the amount of intermetallic layers is limited compared with the interconnections, Ag content of the liquid can be assumed to be constant. Therefore, for an interconnection with the original composition at *a*, the liquid composition after the formation of Cu_6Sn_5 is shifted to *b* at 230°C and varies along *b-b'* with temperature. Fig. 2 shows the calculated x_{Cu} as functions of temperature for interconnections with different silver contents x_{Ag}=0.0065, 0.01, and 0.02.

In the above, it is assumed that Ag_3Sn cannot form before the nucleation of β-Sn, which is true for interconnections with low silver content. Fig.3 shows the temperature at which the driving force for independent β-Sn or Ag_3Sn nucleation appears. The temperature for β-Sn is between 210 and 230°C, whereas the temperature for Ag_3Sn remains lower than 170°C until Ag content exceeds 0.02.

In interconnections with high Ag content, in contrast, β-Sn nucleation may occur either before or after Ag_3Sn formation. Owing to insufficient data for Ag_3Sn formation, the competition between β-Sn and Ag_3Sn nucleation cannot be simulated. The problem can be circumvented, however, by investigating the β-Sn nucleation under two different conditions: 1) Ag_3Sn does not nucleate before β-Sn and the liquid composition varies in the same manner as interconnections with low Ag content; 2) Ag_3Sn forms as long as there is driving force for its nucleation, and the liquid composition vary along *c-c'* rather than *b-b'* in Fig.1 because there is a three-phases (liquid, Ag_3Sn, Cu_6Sn_5) equilibrium. The temperature range for the initiation of solidification can be then determined by combining these two simulated results. Fig.4 shows the calculated liquid composition under the two conditions when x_{Ag}=0.035.

FREE ENERGY OF NUCLEATION

In nucleation, the solder system has to overcome a certain energy barrier, known as the free energy of nucleation. In classical nucleation theory [4,5], the free energy of nucleation is

$$\Delta G = \frac{16}{3}\frac{\pi\sigma^3}{\Delta g^2} \tag{1}$$

where σ is the interfacial energy of the solid/liquid interface, Δg is the Gibbs free energy difference between liquid and solid per unit volume. Accordingly, only those nuclei having sizes larger than a critical value can grow successfully and become effective nuclei, which initiate solidification. The critical size of nucleus, r^*, is

$$r^* = -\frac{2\sigma}{\Delta g} \tag{2}$$

Since σ and Δg determine the free energy of nucleation, their values for liquid solders are discussed in this section.

1) Gibbs Free Energy Difference Δg

The free energy change occurring during solidification is the sum of the chemical potential differences between solid and liquid for all the components. For pure metal, it equals the change in chemical potential per mole $\Delta\mu$ divided by the molar volume V_m of solid

$$\Delta g = \Delta\mu / V_m \tag{3}$$

For a multi-component alloy, average values can be used for the quantities involved. For a near-eutectic SnAgCu solder system,

$$\Delta g = \left(x_{Sn}^S \Delta\mu_{Sn} + x_{Ag}^S \Delta\mu_{Ag} + x_{Cu}^S \Delta\mu_{Cu} \right) \Big/ \overline{V_m} \tag{4}$$

Here $\Delta\mu_i$ is the change in chemical potential for a component i, and x_i^S is the mole fraction of the component i in β-Sn. Since the solubility of Ag and Cu in β-Sn is negligible, Equation (4) is simplified to

$$\Delta g \approx \Delta\mu_{Sn} / V_m = \left(\mu_{Sn}^S - \mu_{Sn}^L \right) / V_m \tag{5}$$

with μ_{Sn}^S and μ_{Sn}^L denoting the chemical potential of Sn in solid and liquid, respectively. It is to be noticed that the chemical potential μ_{Sn}^L depends on the composition of liquid phase as shown above, while the chemical potential μ_{Sn}^S can be regarded as constant at a certain temperature because of low silver and copper contents in β-Sn. Fig.5 shows the calculated Δg values with different Ag contents by using the thermodynamic databank system [10].

2) Interfacial Energy σ

In the early 1950's, Turnbull [11] found the solid/liquid interfacial energy σ of pure Sn to be 0.0525 J/m^2 in a study of the nucleation rate of tin droplets. With the same method, the value was later corrected to 0.059 J/m^2 [12]. An alternative way to derive solid/liquid interfacial energy is the depression of melting point method. With this method the interfacial energy of pure Sn was found to be 0.062±0.01 J/m^2 [13] or 0.069±0.006 J/m^2 [14]. Since the nucleation rate method tends to underestimate σ [15], the latter two values are believed to be more reliable.

Not only are there large errors in experimental measurements of the solid/liquid interfacial energy, there is no way to determine its temperature dependence. Theoretical models [16-18] can be utilized to overcome this problem. With Miedema's model [18], the interfacial energy of pure Sn is presented as a linear function of temperature

$$\sigma = 0.027 + 7.723 \times 10^{-5} T \tag{6}$$

This equation gives a value of 0.066 J/m^2 at the melting point 232°C and a value of 0.058 J/m^2 at 132°C. Considering that the supercooling was about 100°C in nucleation frequency measurements [11], equation (6) is consistent with most of the data reported in literature and provides, therefore, a good description of the interfacial energy σ for pure tin.

The difference in composition at the interface between β-Sn and liquid solder introduces an extra contribution to the interfacial energy. Since the contents of Ag and Cu in SnAgCu solder are low, however, this contribution can be neglected and equation (6) is adopted in the kinetic simulation.

The free energy of nucleation ΔG and the critical nucleus size r^* for β-Sn formation can now be calculated by combining Gibbs free energy difference Δg in

Fig.5 and the interfacial energy σ in equation (5). The results are plotted in Fig.6 and Fig.7.

NUCLEATION RATE

Two mechanisms of nucleation exist in supercooled liquid: homogeneous and heterogeneous nucleation. According to our calculation, however, the homogeneous nucleation rate is very low in solder interconnections, well below $10^{-70}s^{-1}$ at 170°C, which is already 50°C lower than the equilibrium solidification temperature. Homogeneous nucleation of β-Sn can, therefore, hardly occur in solder interconnections during reflow soldering and heterogeneous nucleation at the Liq/Cu_6Sn_5 interfaces is the only mechanism of initiating solidification of interconnections. Hence, we concentrate on heterogeneous nucleation rate in solder interconnections in this section.

The heterogeneous nucleation rate is expressed by the exponential kinetic expression

$$I_{heter} = I^0_{heter} \exp\left(-\frac{\Delta G}{k_B T} f(\theta) \right) \quad (7)$$

where k_B is the Boltzmann's constant, I^0_{heter} is a pre-exponential coefficient and T is temperature. The activation energy is the free energy of nucleation ΔG discussed above.

In Equation (7), $f(\theta)$ is a function of the contact angle θ of the nucleus on a catalytic solid surface. When the catalytic surface is flat, $f(\theta)$ is written as

$$f(\theta) = \frac{1}{4}(2 + \cos\theta)(1 - \cos\theta)^2 \quad (8)$$

If the interconnection does not contain any other impurities or foreign particles, the only site for heterogeneous nucleation is the Liq/Cu_6Sn_5 interface.

Together with the free energy of nucleation presented in the previous section, the pre-coefficient I^0_{heter} and the contact angle θ need to be known in the simulation of nucleation rate.

1) Pre-coefficient I^0_{heter}

The coefficient I^0_{heter} can be calculated as [5]

$$I^0_{heter} = \frac{n_s k_B T}{h} \exp\left(-\frac{\Delta G_A}{k_B T} \right) \quad (9)$$

where h is Plank's constant and n_s is the number of atoms involved in nucleation. ΔG_A is the activation free energy for transporting an atom across the interface, which is approximately the same as the activation energy for viscous flow of liquid.

According to Seetharaman and Sichen [19], the activation energy for viscous flow of liquid alloy can be computed by the equation

$$\Delta G_A = \sum x_i \Delta G_{A,i} + \Delta^m G_{mix} + 3RT \cdot \sum\sum x_i x_j \quad (10)$$

where x is the mole fraction of each component, $\Delta G_{A,i}$ is the activation energy of liquid pure metal i and $\Delta^m G_{mix}$ is the excess Gibbs energy of mixing. ΔG_A is therefore dependent on both temperature and liquid composition. Again with use of the thermodynamic databank system, ΔG_A for different silver contents of interconnections are plotted in Fig. 8.

Assuming a simple cubic arrangement of interfacial atoms, n_s can be calculated as

$$n_s = A \cdot \left(\frac{V_m}{N} \right)^{-2/3} \quad (11)$$

where V_m is the molar volume of liquid and A is the area of the Liq/Cu_6Sn_5 interface. Because of the scallop-type growth of the Cu_6Sn_5 layer during soldering, A is not equal to the projected interfacial area A^* and a factor λ should be added.

$$A = \lambda A^* \quad (12)$$

For SnPb solder, Zuruzi et al. [8] have reported that λ increases from 25 to 60 with increase in soldering time. Assuming that similar Cu_6Sn_5 morphology appears in SnAgCu interconnections, λ is set to be 25 in the simulation.

For a solder droplet on a copper pan in DSC measurement [3], the projected contact area between the solder droplet and the copper pan is approximately $5\times10^{-6}m^2$, while for typical solder interconnections the sum of the upper and lower solder/metallization interfacial areas is about $2\times10^{-7}m^2$. The kinetic simulation below is performed for these values of A^*, $5\times10^{-6}m^2$ and $2\times10^{-7}m^2$.

2) Contact Angle θ

No data is available for the contact angle θ of a β-Sn nucleus at the Liq/Cu_6Sn_5 interface. Theoretically, the balance of three interfacial tensions, $\sigma_{Sn/L}$, σ_{L/Cu_6Sn_5} and σ_{Sn/Cu_6Sn_5}, decides the value of the contact angle θ:

$$\cos\theta = \frac{\sigma_{L/Cu_6Sn_5} - \sigma_{Sn/Cu_6Sn_5}}{\sigma_{Sn/L}} \quad (13)$$

Unfortunately neither σ_{L/Cu_6Sn_5} nor σ_{Sn/Cu_6Sn_5} is known exactly. Some theoretical models might be used to evaluate them, but the error goes completely out of control when the values are subtracted from each other, so that the contact angle cannot be estimated by this means. Instead, we simply apply different values of θ in the simulation and an estimate of θ will be obtained afterwards on the basis of a DSC measurement of the supercooling of solder droplets in a copper pan.

Fig.9 presents the simulated nucleation rates, with different contact angles, nominal contact areas, and silver contents.

ACTUAL SOLIDIFICATION TEMPERATURE

The simulated nucleation rates exhibit typical exponential-type variation over temperature. When the level of supercooling is low, the nucleation rate is so small that solidification is practically impossible. This situation prevails unless the temperature is below a critical range, where the nucleation rate ramps up by many orders of magnitude. In contrast to the equilibrium solidification temperature, the temperature at which solidification occurs is referred as the actual solidification temperature in this paper.

A critical value, I^*, can be assumed to exist as the lowest nucleation rate required for initiating solidification. The value of I^* may be dependent on many factors and difficult to determine exactly. However, since even a small temperature fluctuation changes the rate of nucleation by several orders of magnitudes in the corresponding critical temperature range, only a rough estimate of I^* is sufficient for determining the actual solidification temperature.

Judging by the physical meaning of I^*, it should not depend on the size or composition of the liquid droplets nor on the mechanism of nucleation. Experimentally determined actual solidification temperatures of tin droplets in literature can be therefore utilised to evaluate the scale of I^*. Vonnegut [2] observed that tin droplets ranging in diameters from 1μm to 10μm solidify at 125-132°C. An additional simulation of the homogeneous nucleation rate in tin droplets, as shown in Fig.10, was therefore performed. As the figure shows, 125-132°C corresponds to the nucleation rates from 10^{-14} to 10^{-7} s^{-1}. If we calculate the nucleation rate for 1 mol of liquid, the corresponding values will be 10^{-2} to 10^{5} $s^{-1}mol^{-1}$, which is taken as the critical range of nucleation rate I^*.

The actual solidification of solder interconnections still cannot be estimated without knowing the exact value of the contact angle θ, which strongly influences the simulated nucleation rate as shown in Fig. 9a. In a recent DSC measurement [3], the solidification temperature of a SnAgCu solder droplet on a copper pan was found to lie between 204 and 208°C. The composition of the solder was Sn0.61Ag0.4Cu (x_{Ag}=0.065) and the sample weights 6-12 mg, spreading over an area of approximately $5\times10^{-6}m^2$ on the copper pan. The simulated nucleation rate with x_{Ag}=0.065, $A^*=5\times10^{-6}m^2$ and θ=40° (Fig. 9b) obtains a value between 10^{-2} to 10^{5} $s^{-1}mol^{-1}$ at 205-207°C, which is comparable to the measured solidification temperature. Hence, the contact angle θ of the β-Sn nucleus on Cu_6Sn_5 is assumed in the following to be 40°.

Finally, the estimated critical nucleation rate and contact angle for heterogeneous nucleation of β-Sn at Liq/Cu_6Sn_5 interfaces allow us to predict the actual solidification temperatures of interconnections, as listed in Table.1. The solidification temperature decreases with the increase of Ag content. Since the liquid compositions of interconnections vary with temperature, and since the equilibrium solidification temperature depends on composition, the supercooling levels are calculated with use of the instantaneous equilibrium soldification temperature. As seen in Table 1, the supercooling level decreases slightly with the increase in the silver content, especially when the silver content is low.

Table 1. Predicted Solidification Temperature and Supercooling Level of Solder Interconnection.

	Mole concentration of Ag in interconnection			
	0.0065	0.01	0.02	0.035*
Actual solidification temperature (°C)	205-207	204-206	201-203	198-201
Equilibrium temperature at the actual solidification temperature (°C)	226-230	~225	~222	218-220
Supercooling level at the actual solidification temperature (°C)	21-23	19-21	19-21	19-20
Temperature at which liquid interconnection becomes supercooled with respect to β-Sn (°C)	225	224	221	217
Extent of supercooling during reflow soldering (°C)	18-20	18-20	18-20	17-20

* The temperature range for this composition is the combination of the predicted temperature ranges under two different conditions: with and without Ag_3Sn formation before the nucleation of β-Sn.

However, if the temperature at which the liquid interconnection becomes supercooled with respect to β-Sn is considered, approximately the same temperature range at which interconnections are supercooled during reflow soldering, 18-20°C, is obtained. The equilibrium temperatures at which supercooling commences is determined by calculating thermodynamically the β-Sn+Cu_6Sn_5 binary eutectic monovariant line in the SnAgCu phase diagram and has been presented in Fig.3.

Thus, the actual solidification temperatures of solder interconnections can be directly estimated from the phase equilibria information as shown in Fig.11.

DISCUSSION

The influences of cooling rate, interconnection size, morphology of the intermetallic layer, and component metallizations or boards/metal finishes on the actual solidification temperature are discussed below.

1) Cooling rate

The nucleation rate in Equation (7) is a function of temperature and not related to cooling rate. Since a certain period of time is always required to initiate solidification and since faster cooling rate causes a greater temperature drop, the observed starting point of solidification during continuous cooling is dependent on the cooling rate. This is probably the main reason why the critical nucleation rate cannot be exactly known and a range of I^* value has to be applied.

For normal cooling rate, however, the range of critical nucleation rates 10^{-2} to 10^5 $s^{-1}mol^{-1}$ is believed to be wide enough to accommodate such variation in cooling rate. It means that the change of cooling rate can only cause a variation of 1-2°C in the predicted solidification temperature. This has also been confirmed in DSC measurements, which showed little difference in solidification temperatures when the cooling rate was 1°C/s and 5°C/s [3]. The cooling rate during reflow soldering varies within just 1-3°C/s, which further limits the influence of cooling rate.

2) Interconnection Size

As discussed above, the heterogeneous nucleation rate of a solder droplet is proportional to the nominal area of the Liq/Cu_6Sn_5 interface. The nominal area A^* for typical solder interconnections is one order smaller than that of the DSC samples, being only about 2×10^{-7} m^2. The difference between the nucleation rates is insignificant, however, compared with the wide range of the critical nucleation rate 10^{-2} to 10^5 $s^{-1}mol^{-1}$. It may be concluded that the actual solidification temperature drops only 0.5-1°C when the nominal interfacial area A^* becomes 10 times smaller.

3) Morphology of the Intermetallic Layer

The simulation of nucleation rates above assumes that the Liq/Cu_6Sn_5 interfaces are flat. This is supported by the fact that the critical size of β-Sn nucleus is in the order of 10^{-8}m except at very low supercooling level as shown in Fig.7, which is by far smaller than the radius of Cu_6Sn_5 grains formed during reflow soldering. It means that Equation (8) is always applicable during the nucleation on interconnections, no matter what kind of morphology of the interfaces has been developed. Hence, the only influence of scallop-type Cu_6Sn_5 growth on the actual solidification temperature may come from the increase of the actual to projected Liq/Cu_6Sn_5 areas ratio λ. For an SnPb interconnection, it is reported that λ increases from 25 at the beginning to 60 after 25 hours above liquidu temperature [9]. Such a small increase in the actual Liq/Cu_6Sn_5 area can only cause negligible variation in the predicted solidification temperature. The morphology of the intermetallic layer has little effect, therefore, on the solidification temperature of the interconnection.

4) Component metallizations and boards/metal finishes

In some cases, the intermetallic compound to be formed at the interfaces is altered for different component metallizations or boards/metal finishes. As an

example, when Ni(P)/Au metallization is used, a large amount of Ni is dissolved in the intermetallic layer and the compound formed is $(Cu,Ni)_6Sn_5$ instead of Cu_6Sn_5 [20]. The composition of the liquid that is in equilibrium with the intermetallic layer differs accordingly. Furthermore, the contact angle θ may also be changed on different nucleating surface of intermetallic compound. As shown in Fig. 9a, the nucleation rate is highly sensitive to the contact angle. In the range 30-50°, 1° difference in the contact angle correlates with 1°C difference in the actual solidification temperature. Nevertheless, the actual solidification temperature of interconnections for different intermetallic layer can be analyzed similarly in the same way presented in this paper, which is an interesting point for further investigations.

The actual solidification temperature of interconnections, therefore, should not be significantly changed with the variation of cooling rate, interconnection size and morphology of Cu_6Sn_5 layer. The prediction in Fig.11 applies as long as the same type of intermetallic compound, Cu_6Sn_5, is formed at the interfaces between bulk solder and component metallizations or boards/metal finishes.

SUMMARY

The nucleation energy for β-Sn formation was evaluated by referring to the thermodynamics of near-eutectic SnAgCu solder droplets on copper surface. Since the homogeneous nucleation rate was found to be extremely low, it follows that the solidification temperatures are controlled by the kinetics of heterogeneous nucleation at Liq/Cu_6Sn_5 interfaces. With the free energy of nucleation available, the nucleation rates could be simulated on the basis of classical nucleation theory. They are presented with as exponential functions of temperature, which increases over many orders of magnitude within a narrow temperature range.

By combining the results of an additional simulation of the homogeneous nucleation rates in tin droplets with measured values of the supercooling of the droplets reported in literature, we estimated a range from 10^{-2} to 10^{5} $s^{-1}mol^{-11}$ as the critical nucleation rates for solidification.

At the same time, using the results of DSC measurements we obtained about 40° for the value of the contact angle for heterogeneous β-Sn nucleation at the Liq/Cu_6Sn_5 interface. From these results the temperature of solidification of liquid solder on copper can be predicted. The extent of the supercooling was found to be more or less constant about 18-20°C. Since the supercooling range was only weakly dependent on cooling rate, interconnection size, and the morphology of intermetallic phases at Liq/Cu_6Sn_5 interfaces, the solidification temperatures of interconnections can be finally predicted on the basis of phase equilibria in the SnAgCu solder system.

Reference

1. J.K.Kivilahti, "The Chemical Modelling of Electronic Materials and Interconnections", Journal of Metals, vol. 54, 2002, No.12, pp. 52-57, 2002.
2. B. Vonnegut, "Variation with Temperature of the Nucleation Rate of Supercooled Liquid Tin and Water Drops", J. Colloid Sci., 3, pp.563-569, 1948.
3. Koivisto, J., M.S. Thesis., Helsinki University of Technology (2004).
4. D.Turnbull, "Formation of Crystal Nuclei in Liquid Metals", Journal of Applied Physics, 21, pp.1022-1028, 1950.
5. B.Cantor and R.D.Doherty, "Heterogeneous Nucleation in Solidifying Alloys", Acta Metallurgica., Vol. 27, pp. 33-46,1979.

6. H.Yu and J.Kivilahti, "CFD Modelling of the Flow Field inside Reflow Oven", Journal of Soldering & Surface Mount Technology, Vol. 14, No. 1, pp. 38-44, 2002.
7. H.Yu, T.T.Mattila and J.K.Kivilahti, "Thermal Simulation of the Solidification of Lead-free Solder Interconnections", to be published in IEEE Transactions on Components and Packaging Technologies.
8. W.Kurz and D.J.Fisher, "Fundamentals of Solidification", Fourth revised edition, Appendix 2, ISBN 0-87849-804-4, Trans Tech Publications Ltd, Switzerland, 1998.
9. A.S.Zuruzi, C.-h.Chiu, S.K.Lahiri and K.N.Tu, "Roughness Evolution of Cu_6Sn_5 Intermetallic during Soldering", Journal of Applied Physics, 86, No.9, 4916-4921, 1999.
10. J.-O.Andersson, T.Helander, L.Höglund, P.F.Shi, and B.Sundman, "Thermo-Calc & DICTRA, Computational Tools for Materials Science", Calphad, Vol.26, No.2, pp. 273-312, 2002.
11. Turbull, B., "Isothermal Rate of Solidification of Small Droplets of Mercury and Tin", J. Chem. Phys., 18, 768 (1950).
12. V.Scripov, "Crystal Growth and Materials", edited by E.Kaldis and H.Scheel, Amsterdam, North-Holland, pp.327, 1977.
13. C.R.M.Wronski, "The Size Dependence of the Melting Point of Small Particles of Tin", Brit. J. Appl. Phys., Vol.18, pp.1731-1737, 1967.
14. R.P.Berman and A.E.Curzon, "The Size Dependence of the Melting Point of Small Particles of Indium", Can. J. Phys., Vol.52, No.11, pp.923-929, 1974.
15. N.Eustathopoulos, "Energetics of Solid/Liquid Interfaces of Metals and Alloys", International Metals Reviews, Vol.28, No.4, pp.189-210, 1983.
16. R.H.Ewing, "The Free Energy of the Crystal-Melt Interface from the Radial Distribution Function", J. Crystal Growth, Vol.11, pp.221-224, 1971.
17. Y.Waseda and W.A.Miller, "Calculation of the Crystal-Melt Interfacial Free Energy from Experimental Radial Distribution Function Data", Trans. Jpn. Inst. Met., 19, 546, 1978.
18. A.R.Miedema and F.J.A.den Broeder, "On the Interfacial Energy in Solid-Liquid and Solid-Solid Metal Combinations", Z.Metallkde., Vol.70, No.1, pp.14-20, 1979.
19. S.Seetharaman and DU Sichen, "Estimation of the Viscosities of Binary Metallic Melts Using Gibbs Energies of Mixing", Metallurgical and Materials Transaction, Vol.25B, pp.589-595, 1979.
20. K. Zeng, V. Vuorinen, and J. K. Kivilahti, " Interfacial Reactions Between Lead-Free SnAgCu Solder and Ni(P) Surface Finish on Printed Circuit Boards", IEEE Transactions on Component, Packaging and Manufacturing Technology, 25, 162, 2002.

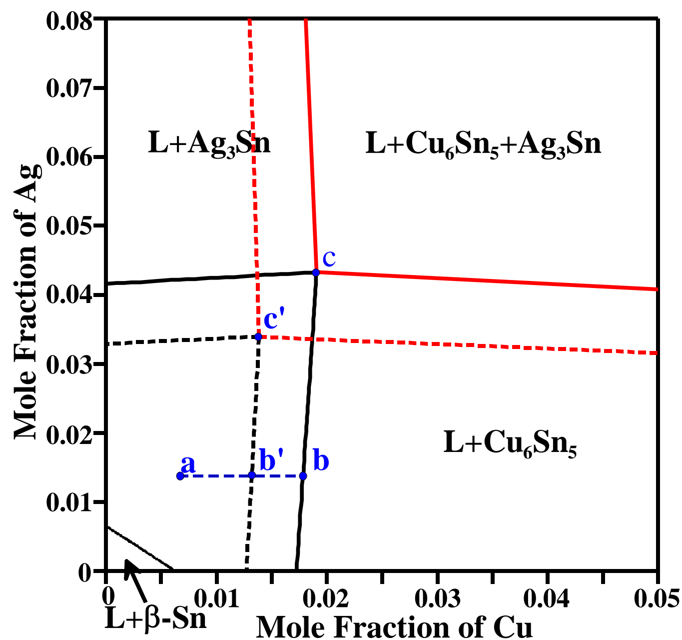

Fig.1 Sn corner of calculated isothermal sections of SnAgCu phase diagram at 230°C (solid line) and210°C (dotted line, β-Sn phase is suspended).

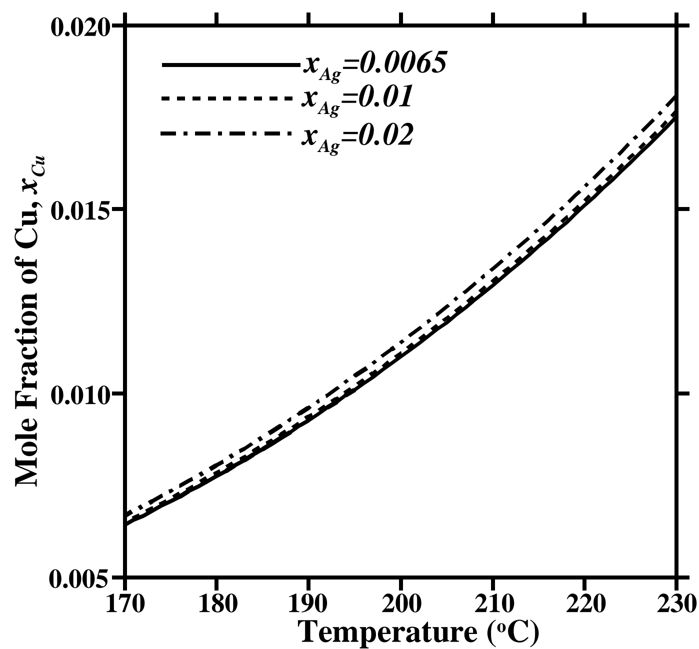

Fig.2 Calculated liquid copper content x_{Cu} of interconnection.

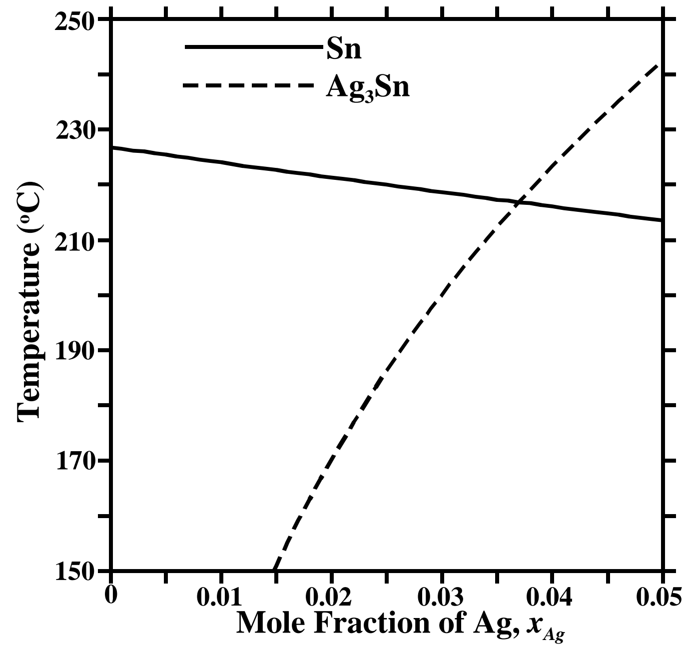

Fig.3 Temperature at which the driving force for independent β-Sn or Ag_3Sn nucleation appears, determined by the calculated temperature of binary eutectic reaction L⇒Cu_6Sn_5+Ag_3Sn (suspending β-Sn) or L⇒Cu_6Sn_5+β-Sn (suspending Ag_3Sn).

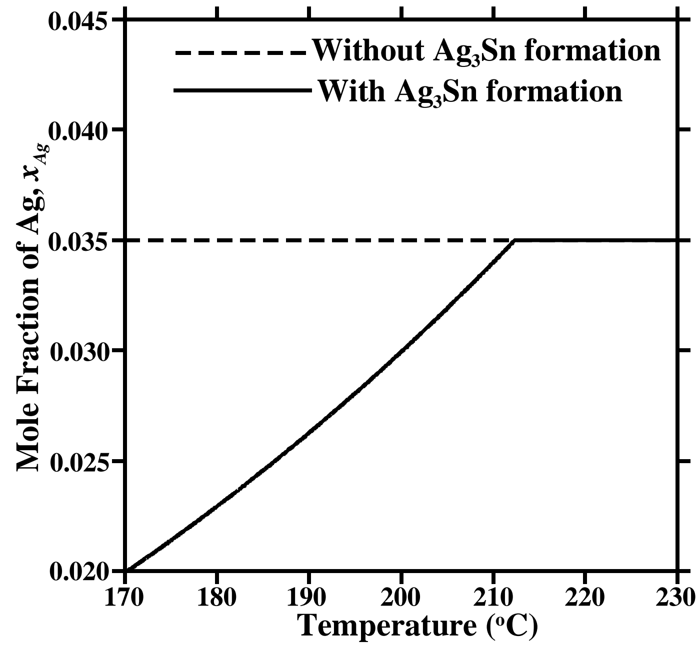

(a)

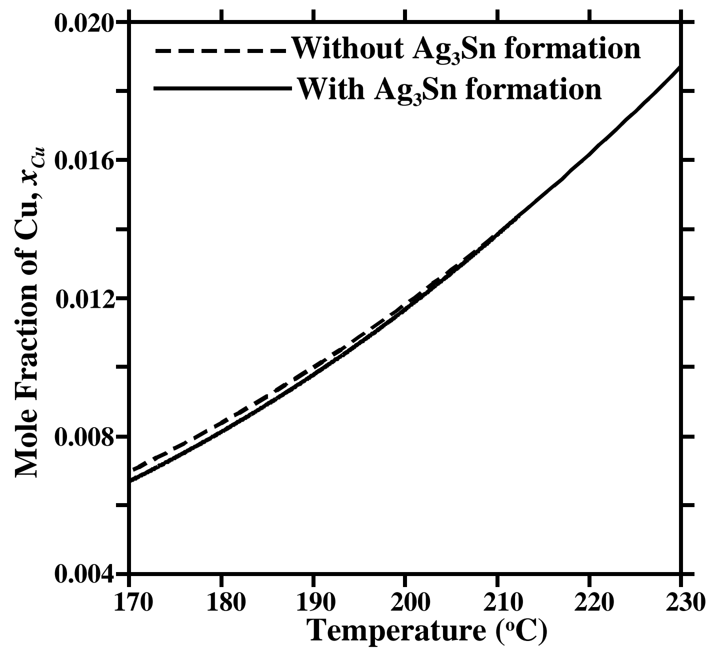

(b)

Fig.4 Calculated liquid composition of interconnection with different assumptions about Ag_3Sn formation. The original Ag content of solder alloy is 0.035.
(a) Silver Content; (b) Copper Content.

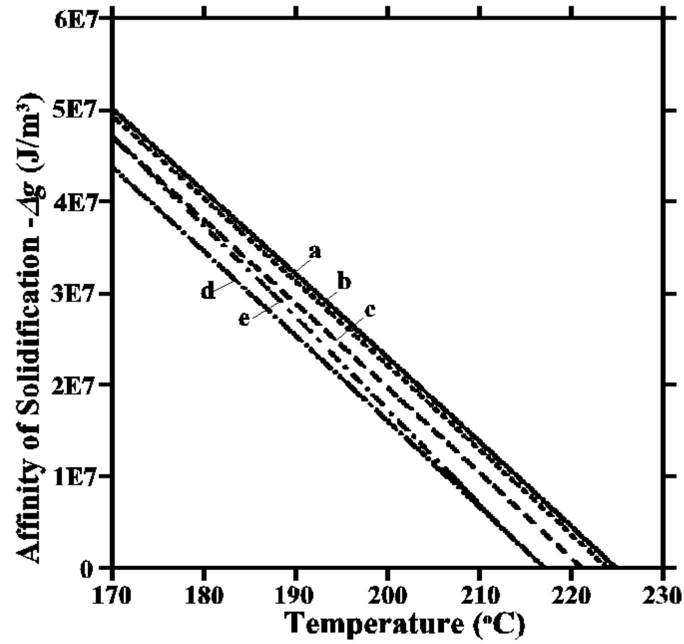

Fig.5 Affinity of solidification (the opposite value of driving force Δg) per unit volume of β-Sn nucleation.

a: x_{Ag} =0.0065; b: x_{Ag} =0.01; c: x_{Ag} =0.02;

d: x_{Ag} =0.035, without Ag_3Sn formation;

e: x_{Ag} =0.035, with Ag_3Sn formation.

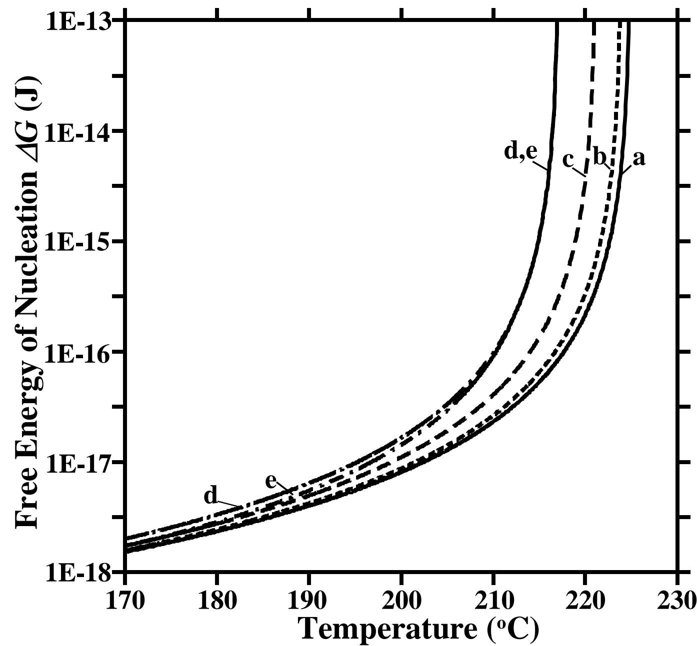

Fig.6 Free energy of nucleation ΔG of β-Sn.

a: x_{Ag} =0.0065; b: x_{Ag} =0.01; c: x_{Ag} =0.02;

d: x_{Ag} =0.035, without Ag_3Sn formation;

e: x_{Ag} =0.035, with Ag_3Sn formation.

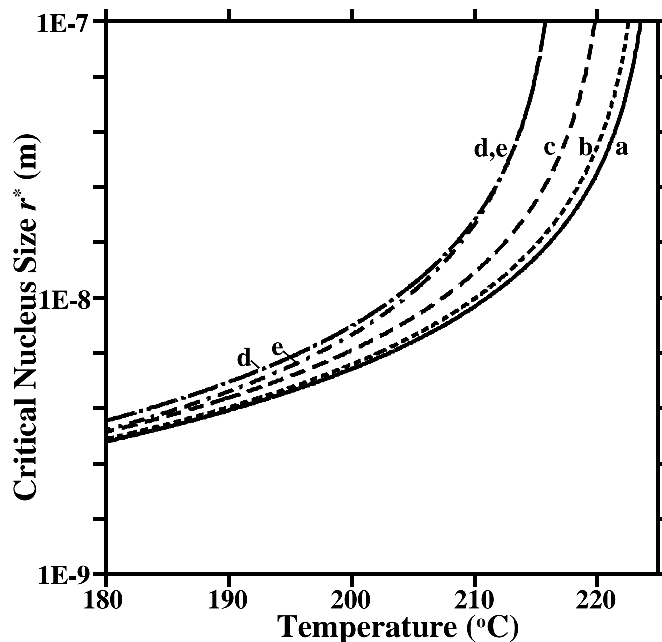

Fig.7 Critical nucleus size r^* of β-Sn nucleation.

a: x_{Ag} =0.0065; b: x_{Ag} =0.01; c: x_{Ag} =0.02;

d: x_{Ag} =0.035, without Ag_3Sn formation;

e: x_{Ag} =0.035, with Ag_3Sn formation.

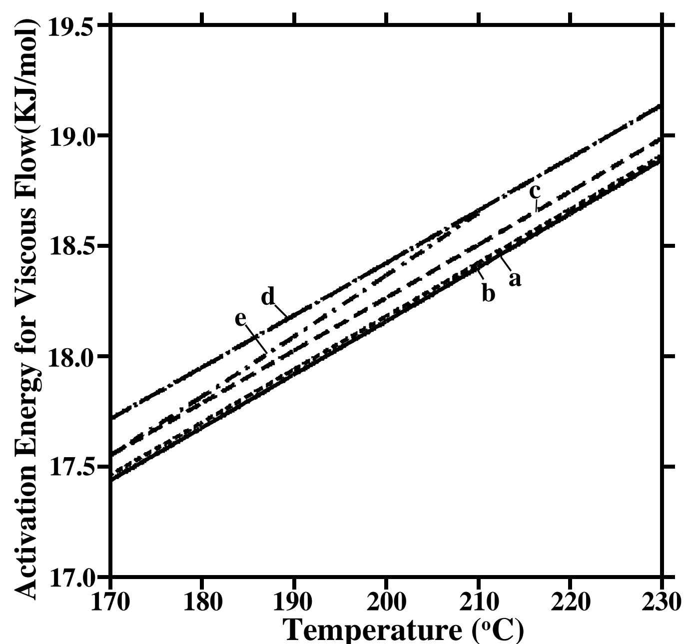

Fig.8 Activation energy for viscous flow of liquid interconnection.

a: x_{Ag} =0.0065; b: x_{Ag} =0.01; c: x_{Ag} =0.02;

d: x_{Ag} =0.035, without Ag_3Sn formation;

e: x_{Ag} =0.035, with Ag_3Sn formation.

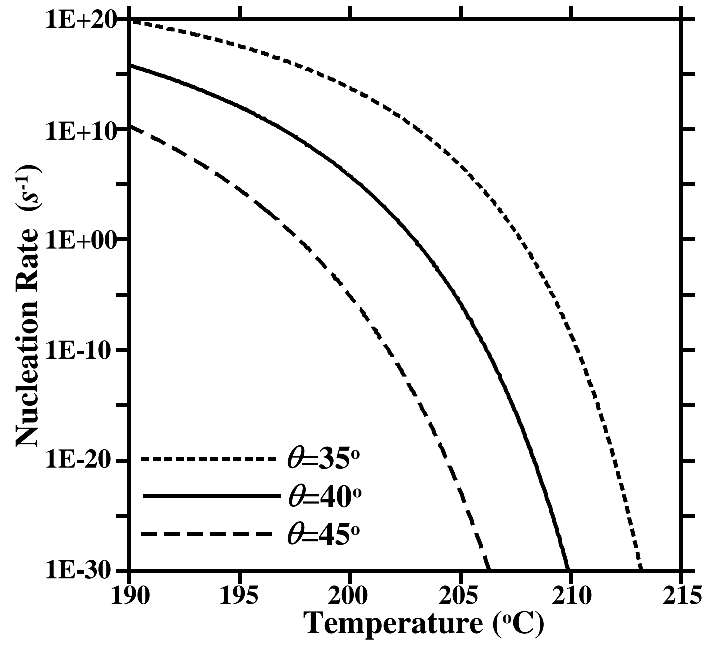

(a)

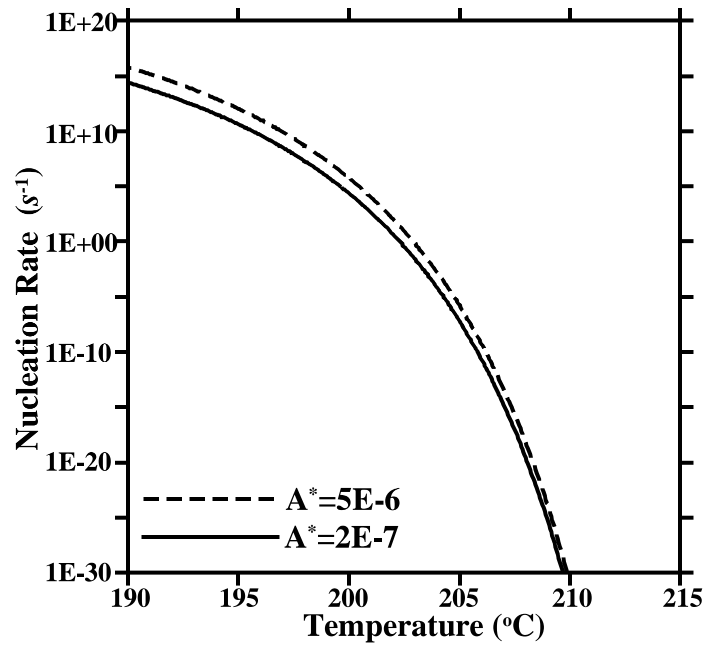

(b)

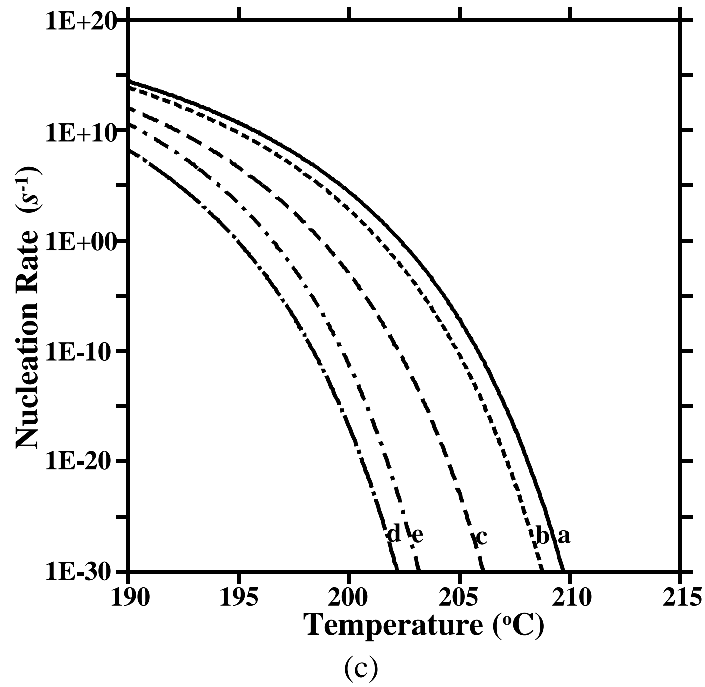

(c)

Fig.9 Some results of calculated nucleation rate, with different assumed contact angle, nominal contact area, and silver content.

(a) Different contact angle, A^{*}=5×10^{-6}m^{2} and x_{Ag}=0.0065;

(b) Different nominal contact area, θ=40° and xAg=0.0065;

(c) Different silver content (a-e marked in the same way as Fig.7), θ=40° and A^{*}=2×10^{-7}m^{2}.

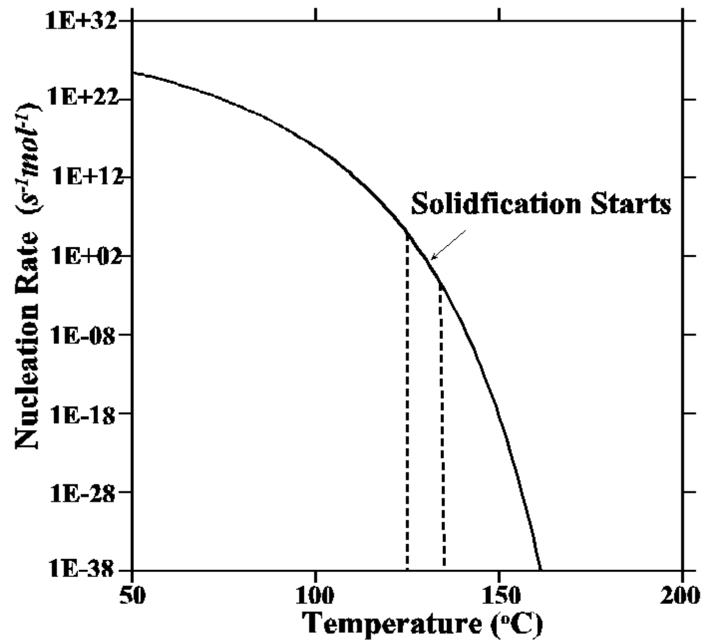

Fig.10 Calculated nucleation rate of pure tin droplet with diameter 5μm.

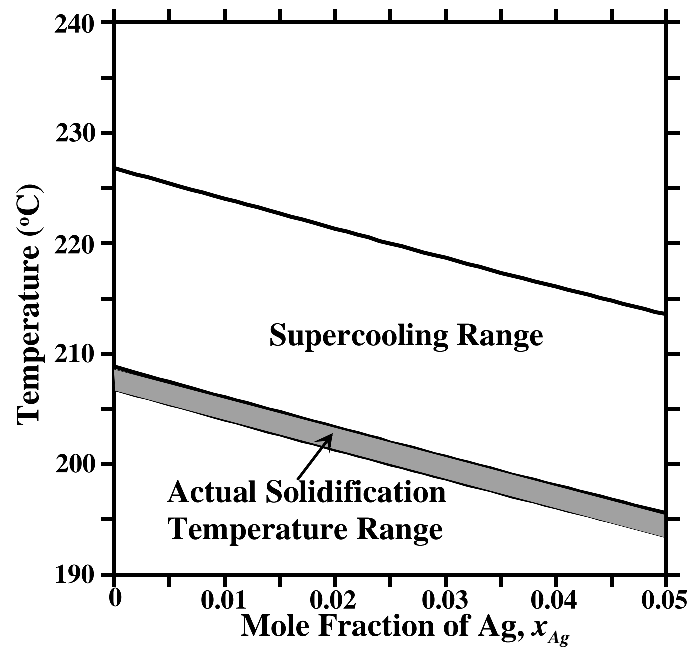

Fig.11 Predicted actual solidification temperature of SnAgCu solder interconnections during reflow soldering.